# CHAPTER 3

## EXPERIMENTAL PROCEDURE

This chapter describes all experimental procedures employed in this work to fabricate and characterize the desired transparent glass-ceramics which contain $LiNbO_3$ ferroelectric nano-crystals using the incorporation method.

### 3.1 Samples preparation

Preparation of $LiNbO_3$ powders, glass and glass-ceramic samples were carried out using the heat treatment method. After that the characterization, of the glasses and glass-ceramics containing $LiNbO_3$ ferroelectric nano-crystals, was performed as described following section:

All commercially available starting compounds used in this study are listed in Table 3.1, along with the suppliers, formula weights and purities.

### 3.1.1 $LiNbO_3$ powder

In this part, all powder compositions were prepared by a solid-state mixed oxide method. In the mixing process, the calculated relevant proportions of constituents were weighed according to the formula below:

$$Li_2CO_{3(s)} + Nb_2O_{5(s)} \rightarrow 2LiNbO_{3(s)} + CO_{2(g)} \qquad \textbf{(3.1)}$$

High purity $Li_2CO_3$ and $Nb_2O_5$ (purity > 99.0%) powders were used as starting materials and mixed with a molar ratio of [Li]/[Nb] = 1:1. To prepare the $LiNbO_3$ source powder via thermal treatment of a stoichiometric mixture of $Li_2CO_3$ and $Nb_2O_5$ within a solid state reaction route at 600-800 °C for 2 h in air to remove the $CO_2$ from $Li_2CO_3$ with a heating and cooling rate of 5 K/min which the results and discussion were shown in appendix. In this research, $LiNbO_3$ powder was calcined at 800 °C for 2 h to be suitable condition.

**Table 3.1** Specifications of the raw materials used for preparation $LiNbO_3$ powder and glass samples.

| Raw materials | Source | Formula weight | Purities (%) |
|---|---|---|---|
| Lithium Carbonate $[Li_2CO_3]^{\#,*}$ | Merck KGaA, Germany | 73.89 | 99.0-100.0 |
| Niobium (V) Oxide $[Nb_2O_5]_{\#,*}$ | Alfa Aesar Gmbh & Co KG, Germany | 265.81 | 99.5 |
| Silicon Oxide $[SiO_2]_*$ | Carl Roth GmbH & Co, Germany | 60.08 | > 99.0 |
| Aluminium Hydroxide $[Al(OH)_3{\cdot}xH_2O]^*$ | Merck KGaA, Germany | 78.0036 | > 99.5 |

# for preparation of $LiNbO_3$ powder

* for preparation of glass samples

### 3.1.2 Glass samples

Glasses in the system (100-$x$)$LiNbO_3 \cdot xSiO_2$ with $10 \leq x \leq 60$ in molar ratio and (95-$x$)$LiNbO_3 \cdot xSiO_2 \cdot 5Al_2O_3$ with $15 \leq x \leq 55$ in molar ratio were prepared from the prepared $LiNbO_3$ (Topic 3.1.1), $SiO_2$ and $Al_2O_3$ as shown in Table 3.2 by incorporation method. Firstly, $LiNbO_3$ was synthesized and then melted with other compositions using the conventional melting technique. The incorporation method may benefit the ease of crystallization of $LiNbO_3$ phase and reduce the chance of any unwanted second phase to occur. These glass systems were chosen by the following reasons: (1) $SiO_2$ is a glass forming oxide that does not modify the $LiNbO_3$ lattice, (2) the use of a large amount of lithium and niobium oxides increases the probability of the higher number of $LiNbO_3$ crystal precipitation [67], (3) the $LiNbO_3$ stoichiometric is suitable for using the equal amount of $Li_2O$ and $Nb_2O_5$, and (4) it is possible to obtain a transparent glass (optical applications) with improved electro-optic applications [6, 73]. The homogeneous mixtures of stoichiometric (in molar ratio) compositions were melted in a platinum crucible in air using a melting electric furnace (Nabertherm, Germany) (Fig. 3.1) at 1300-1450 °C, depending on the composition of the batches, for 1 h to yield 30 g of the glasses. The melts were quenched by pouring onto a brass block (Fig. 3.2) and immediately pressed with another plate to obtain 1.5-2.0 mm thick glass sheets (Fig. 3.3). Subsequently all glass samples under study were annealed at 550 °C for 1 h, to anneal out thermal stresses that are likely to be associated with them, and slowly cooled at the rate of 1 K/min in an annealing electric furnace (Nabertherm, Germany) (Fig. 3.4) to room temperature. Many glass compositions were melted for trial and error in order to find the optimum glass composition, which could be kept into the glassy state by a moderate cooling rate.

**Fig. 3.1** Melting electric furnace.

**Fig. 3.2** Pouring melting glass onto a brass block.

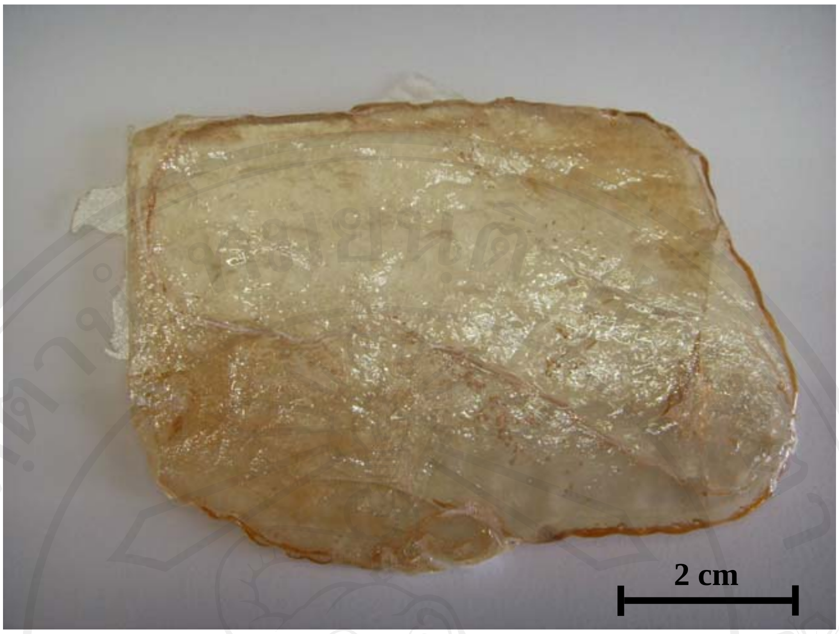

**Fig. 3.3** Glass sample.

**Fig. 3.4** Annealing electric furnace.

**Table 3.2** Chemical compositions of the prepared glass samples.

| **Glass samples** | **Chemical compositions (mol %)** | | |
|---|---|---|---|
| | **$LiNbO_3$** | **$SiO_2$** | **$Al_2O_3$** |
| $90LiNbO_3 \cdot 10SiO_2$ | 90 | 10 | - |
| $80LiNbO_3 \cdot 20SiO_2$ | 80 | 20 | - |
| $75LiNbO_3 \cdot 25SiO_2$ | 75 | 25 | - |
| $70LiNbO_3 \cdot 30SiO_2$ | 70 | 30 | - |
| $65LiNbO_3 \cdot 35SiO_2$ | 65 | 35 | - |
| $60LiNbO_3 \cdot 40SiO_2$ | 60 | 40 | - |
| $55LiNbO_3 \cdot 45SiO_2$ | 55 | 45 | - |
| $50LiNbO_3 \cdot 50SiO_2$ | 50 | 50 | - |
| $40LiNbO_3 \cdot 60SiO_2$ | 40 | 60 | - |
| $80LiNbO_3 \cdot 15SiO_2 \cdot 5Al_2O_3$ | 80 | 15 | 5 |
| $70LiNbO_3 \cdot 25SiO_2 \cdot 5Al_2O_3$ | 70 | 25 | 5 |
| $60LiNbO_3 \cdot 35SiO_2 \cdot 5Al_2O_3$ | 60 | 35 | 5 |
| $50LiNbO_3 \cdot 45SiO_2 \cdot 5Al_2O_3$ | 50 | 45 | 5 |
| $40LiNbO_3 \cdot 55SiO_2 \cdot 5Al_2O_3$ | 40 | 55 | 5 |

### 3.1.3 Glass-ceramic samples

All prepared transparent glass samples were chosen for further controlled crystallization by the heat treatment method. Glass sample sheets were covered by a platinum sheet and heat-treated in the electric furnace (Fig. 3.4). To find a suitable way to control the crystallization of glass samples, in order to obtain the desired ferroelectric crystallization phase, on nano scale, in glassy matrix was one of our purposed in this study. The heat treatment method is of primary importance for types, volume contents and sizes of the obtained crystalline phase.

The glass samples were heat-treated at different temperatures (580, 600, 625, 650, 700 and 975 °C) using a heating and cooling rate of 10 K/min for various periods of time (1, 3 and 6 h) to convert the glasses to glass-ceramics. The transparency of the heat-treated samples was examined only visually; "transparent" means that letters placed beneath the samples could be read through the samples (Fig. 3.5).

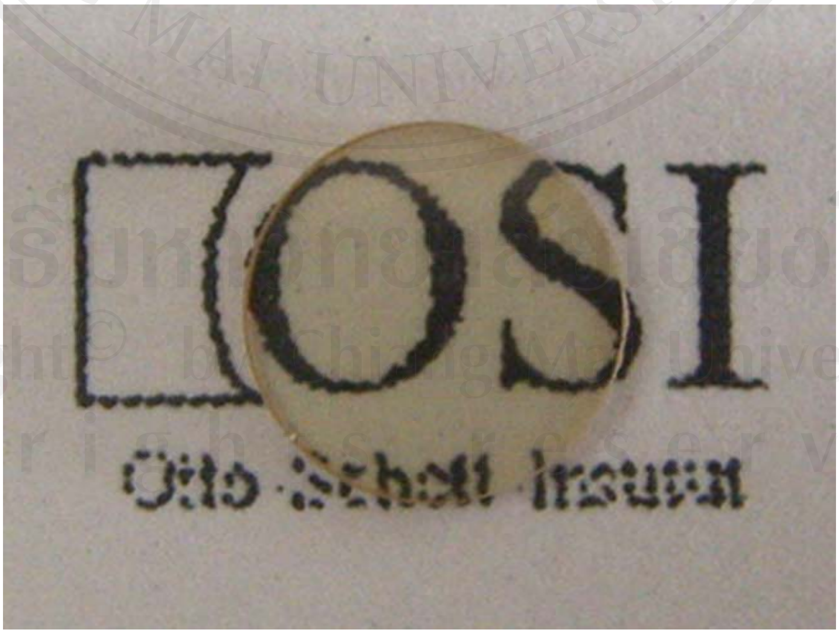

**Fig. 3.5** Transparent glass sample.

## 3.2 $LiNbO_3$ powder, glass and glass-ceramic samples characterization

The following section is intended to address the main characterization techniques used to investigate the thermal analysis and phase analysis of the mixed $Li_2CO_3$ and $Nb_2O_5$ powders were prepared at different temperatures. Then, the glass and glass-ceramic samples in this study also examined the phase formation, morphology, microstructure, thermal analysis, optical and electrical properties.

### 3.2.1 Thermal analysis

Thermal analysis generally covers three different experimental techniques: thermogravimetric analysis (TGA), differential thermal analysis (DTA) and differential scanning calorimetry (DSC). The mixed powders of $Li_2CO_3$ and $Nb_2O_5$, all glasses and glass-ceramics were ground into powders, placed in the platinum crucible about 30 mg. In this research, thermogravimetric analyzer (TGA 50, Shimadzu, Germany) (Fig. 3.6) and differential thermal analyzer (DTA 50, Shimadzu, Germany) (Fig. 3.7) was used in the 30-1350 °C temperature range. A heating rate of 10 K/min was carried out to determine the average value of the weight loss and glass transition temperatures ($T_g$), crystallization temperatures ($T_{Cr}$) and melting temperatures ($T_m$) [74].

Many thermal changes in glass samples (e.g. phase transitions) do not involve a change of mass. In DTA one instead measures the temperature difference between an inert reference and the glass samples as a function of temperature. When the samples undergo a physical or chemical change, the temperature increase differently between the inert reference and the glass samples and a peak or a dip then is detected in the DTA signal. The technique is routinely applied in a wide range of studies such as identification, quantitative composition analysis, phase diagrams, hydration-dehydration, thermal stability, polymerization, purity, and reactivity [75].

**Fig. 3.6** Thermogravimetric analyzer.

**Fig. 3.7** Differential thermal analyzer.

### 3.2.2 Densification analysis

The bulk density was determined for all glass and glass-ceramic samples, the weight was measured using a balance (Analytic AC 210 P, Sartorius, Germany) with density equipment (Fig. 3.8) as recommended by the ASTM C 20-00 [76]. The bulk density ($\rho_b$) was calculated using Archimedes' principle according to the equation as follows:

$$\rho_b = \frac{W_D}{V_b} \tag{3.2}$$

Where $W_D$ is the dry weight of specimen and $V_b$ is the bulk volume.

The density ($\rho$) of the immersed object relative to the density of the fluid ($\rho_{Fluid}$) at that temperature can easily be calculated without measuring any volumes [77]:

$$\rho = \frac{W_{Air}}{W_{Air} - W_{Fluid}} \bullet \rho_{Fluid} \ (at\ that\ temperature) \tag{3.3}$$

Where $W_{Air}$ is the weight in air of the specimen and $W_{Fluid}$ is the weight in fluid of the specimen. In this research, the glass and glass-ceramic samples were measured with distilled water as the immersion liquid (fluid). The density of distilled water at that temperature is shown in Table 3.3.

The true densities of the specimens were measured using a nitrogen (N) pycnometer (AccuPyc 1330, Micromeritics Instrument Corp, Norcross, USA) (Fig. 3.9).

**Table 3.3** The density of the fluid (distilled water) at various temperatures (To be continued). [78]

| Temperature (°C) | 0 | 0.1 | 0.2 | 0.3 | 0.4 | 0.5 | 0.6 | 0.7 | 0.8 | 0.9 |
|---|---|---|---|---|---|---|---|---|---|---|
| **0** | 0.999841 | 0.999847 | 0.999854 | 0.999860 | 0.999866 | 0.999872 | 0.999878 | 0.999884 | 0.999889 | 0.999895 |
| **1** | 0.999900 | 0.999905 | 0.999909 | 0.999914 | 0.999918 | 0.999923 | 0.999927 | 0.999930 | 0.999934 | 0.999938 |
| **2** | 0.999941 | 0.999944 | 0.999947 | 0.999950 | 0.999953 | 0.999955 | 0.999958 | 0.999960 | 0.999962 | 0.999964 |
| **3** | 0.999965 | 0.999967 | 0.999968 | 0.999969 | 0.999970 | 0.999971 | 0.999972 | 0.999972 | 0.999973 | 0.999973 |
| **4** | 0.999973 | 0.999973 | 0.999973 | 0.999972 | 0.999972 | 0.999972 | 0.999970 | 0.999969 | 0.999968 | 0.999966 |
| **5** | 0.999965 | 0.999963 | 0.999961 | 0.999959 | 0.999957 | 0.999955 | 0.999952 | 0.999950 | 0.999947 | 0.999944 |
| **6** | 0.999941 | 0.999938 | 0.999935 | 0.999931 | 0.999927 | 0.999924 | 0.999920 | 0.999916 | 0.999911 | 0.999907 |
| **7** | 0.999902 | 0.999898 | 0.999893 | 0.999888 | 0.999883 | 0.999877 | 0.999872 | 0.999866 | 0.999861 | 0.999855 |
| **8** | 0.999849 | 0.999843 | 0.999837 | 0.999830 | 0.999824 | 0.999817 | 0.999810 | 0.999803 | 0.999796 | 0.999789 |
| **9** | 0.999781 | 0.999774 | 0.999766 | 0.999758 | 0.999751 | 0.999742 | 0.999734 | 0.999726 | 0.999717 | 0.999709 |
| **10** | 0.999700 | 0.999691 | 0.999682 | 0.999673 | 0.999664 | 0.999654 | 0.999645 | 0.999635 | 0.999625 | 0.999615 |
| **11** | 0.999605 | 0.999595 | 0.999585 | 0.999574 | 0.999564 | 0.999553 | 0.999542 | 0.999531 | 0.999520 | 0.999509 |
| **12** | 0.999498 | 0.999486 | 0.999475 | 0.999463 | 0.999451 | 0.999439 | 0.999427 | 0.999415 | 0.999402 | 0.999390 |
| **13** | 0.999377 | 0.999364 | 0.999352 | 0.999339 | 0.999326 | 0.999312 | 0.999299 | 0.999285 | 0.999272 | 0.999258 |
| **14** | 0.999244 | 0.999230 | 0.999216 | 0.999202 | 0.999188 | 0.999173 | 0.999159 | 0.999144 | 0.999129 | 0.999114 |
| **15** | 0.999099 | 0.999084 | 0.999069 | 0.999054 | 0.999038 | 0.999023 | 0.999007 | 0.998991 | 0.998975 | 0.998959 |

**Table 3.3** The density of the fluid (distilled water) at various temperatures.

| **Temperature (°C)** | **0** | **0.1** | **0.2** | **0.3** | **0.4** | **0.5** | **0.6** | **0.7** | **0.8** | **0.9** |
|---|---|---|---|---|---|---|---|---|---|---|
| **16** | 0.998943 | 0.998926 | 0.998910 | 0.998893 | 0.998877 | 0.998860 | 0.998843 | 0.998826 | 0.998809 | 0.998792 |
| **17** | 0.998774 | 0.998757 | 0.998739 | 0.998722 | 0.998704 | 0.998686 | 0.998668 | 0.998650 | 0.998632 | 0.998613 |
| **18** | 0.998595 | 0.998576 | 0.998558 | 0.998539 | 0.998520 | 0.998501 | 0.998482 | 0.998463 | 0.998444 | 0.998424 |
| **19** | 0.998405 | 0.998385 | 0.998365 | 0.998345 | 0.998325 | 0.998305 | 0.998285 | 0.998265 | 0.998244 | 0.998224 |
| **20** | 0.998203 | 0.998183 | 0.998162 | 0.998141 | 0.998120 | 0.998099 | 0.998078 | 0.998056 | 0.998035 | 0.998013 |
| **21** | 0.997992 | 0.997970 | 0.997948 | 0.997926 | 0.997904 | 0.997882 | 0.997860 | 0.997837 | 0.997815 | 0.997792 |
| **22** | 0.997770 | 0.997747 | 0.997724 | 0.997701 | 0.997678 | 0.997655 | 0.997632 | 0.997608 | 0.997585 | 0.997561 |
| **23** | 0.997538 | 0.997514 | 0.997490 | 0.997466 | 0.997442 | 0.997418 | 0.997394 | 0.997369 | 0.997345 | 0.997320 |
| **24** | 0.997296 | 0.997271 | 0.997246 | 0.997221 | 0.997196 | 0.997171 | 0.997146 | 0.997120 | 0.997095 | 0.997069 |
| **25** | 0.997044 | 0.997018 | 0.996992 | 0.996967 | 0.996941 | 0.996914 | 0.996888 | 0.996862 | 0.996836 | 0.996809 |
| **26** | 0.996783 | 0.996756 | 0.996729 | 0.996703 | 0.996676 | 0.996649 | 0.996621 | 0.996594 | 0.996567 | 0.996540 |
| **27** | 0.996512 | 0.996485 | 0.996457 | 0.996429 | 0.996401 | 0.996373 | 0.996345 | 0.996317 | 0.996289 | 0.996261 |
| **28** | 0.996232 | 0.996204 | 0.996175 | 0.996147 | 0.996118 | 0.996089 | 0.996060 | 0.996031 | 0.996002 | 0.995973 |
| **29** | 0.995944 | 0.995914 | 0.995885 | 0.995855 | 0.995826 | 0.995796 | 0.995766 | 0.995736 | 0.995706 | 0.995676 |
| **30** | 0.995646 | 0.995616 | 0.995586 | 0.995555 | 0.995525 | 0.995494 | 0.995464 | 0.995433 | 0.995402 | 0.995371 |

**Fig. 3.8** Balance with density equipment.

**Fig. 3.9** Pycnometer.

### 3.2.3 Phase analysis

#### 3.2.3.1 X-ray diffractrometry

X-ray diffraction (Diffractometer D 5000, Siemens, Germany) (Fig. 3.10) analysis was conducted to determine the crystalline phase formation within $LiNbO_3$ powders and the glass composite materials. $LiNbO_3$ powders, all glass and glass-ceramic samples were ground into powders, placed in the holder of a diffractometer and scanned with CuKα radiation, 1.5418 Å, λ at 45 kV and 40 mA. In addition, diffraction patterns were collected in the 2theta (2θ) ranging from 10° to 60° with step size of 0.02° per second. The phases shown in the diffraction patterns were compared against the Joint Committee of Powder Diffraction Standard (JCPDS) database, in order to determine the phase existed in the samples.

**Fig. 3.10** X-ray diffractometer.

The crystallite size was estimated using the Scherrer equation: [79, 80]

$$\beta_{crystalline} = \frac{k\lambda}{L\cos\theta} \tag{3.4}$$

Where $\beta_{crystalline}$ is the full width at half maximum (FWHM, obtained for high intense peak, in the present studies), $k$ is a constant which is usually varies in the range from 0.89 to 1.00, depending on the crystalline shape, in this study $k = 0.94$, $\lambda$ is the wavelength used (1.5406 Å), $L$ is the "average" crystallite size measured in a direction perpendicular to the surface of the specimen and $\theta$ is the Bragg angle.

### 3.2.3.2 Raman Spectroscopy

In achievement of network structure information of amorphous and crystalline lithium niobate, Raman spectroscopy (Raman spectrometer; Jobin-Yvon T64000 triple monochromator, Horiba, Japan) (Fig. 3.11) has taken an advantage in structural determination. Glass samples were finely polished (1 µm). Then, the samples were placed on a glass slide in order to characterize the response of molecules to energy. Raman scattering data was collected by a microscope equipped with 100x lenses using 514.5 nm exciting light of an argon laser operating at 50 mW. The acquisition time required for the recording of each spectrum was 120 seconds.

**Fig. 3.11** Raman spectrometer.

### 3.2.4 Microstructural analysis

Polished glass and glass-ceramic samples (with diamond paste from 9 to 1 µm) were etched with 1 mol % of hydrofluoric acid (HF) for 2 min and gold (Au)-coated for scanning electron microscope (SEM) observations with field emission SEM (JSM 6335 F, Jeol, Tokyo, Japan) equipped with an energy dispersive X-ray analyzer (EDX) (Fig. 3.12). The chemical composition of the significant microstructural features was also analyzed using an EDX technique.

Glass samples were further investigated by transmission electron microscope (TEM; H 8100, Hitachi, Japan) (Fig. 3.13) using an acceleration voltage of 200 kV. The following replica technique was used. The glass samples were fractured in vacuum and coated with a thin Pt-Ir-C layer. After treatment with acid, the film was removed from the surface and studied by TEM (for a detailed description see [81]). The replica film shows only the topography of the fractured surface and is not affected by the etching procedure.

**Fig. 3.12** Scanning electron microscope, equipped with EDX analyzer.

**Fig. 3.13** Transmission electron microscope.

### 3.2.5 Measurement of optical properties

#### 3.2.5.1 Transmittance (%)

In this research, the glass and glass-ceramic samples were polished to optical quality on both surfaces in order to obtain a sample thickness 1 mm and diameter 6 mm as same as the sample in Fig. 3.5. The optical transmission spectra were measured using an ultraviolet-visible-near infrared (UV-Vis-NIR) spectrophotometer (UV-3101PC, Shimadzu, Germany) (Fig. 3.14) in the range of 350 to 2500 nm.

Inside a spectrophotometer, light of a specific wavelength shines on a sample that is usually liquid. The sample contains a substance of interest, the analytic. As the light passes through the sample, some of its energy is absorbed by the analyst while the rest passes through. The light that passes through without being absorbed is called “transmitted light”. The spectrophotometer has a detector that is sensitive to transmitted light. A blank is a reference solution that contains no analyzes but does contain the solvent and any reagents that are intentionally added to the sample. The spectrophotometer compares the interaction of light with the sample and with a blank in order to establish the effect of the analyst. Transmittance is defined as [82]:

$$\frac{\textit{Light transmitted through the sample}}{\textit{Light transmitted through the blank}} = \textit{Transmittance} = t \qquad \textbf{(3.5)}$$

Percent transmittance is the transmittance time 100%:

$$\%T = t \times 100\,\% \qquad \textbf{(3.6)}$$

Transmittance or percent transmittance can range from 0 or 0% (no light passes through the sample relative to the blank) to 1 or 100% (all light passes through). All spectrophotometers actually measure transmittance which is the ratio between the amount of light transmitted through a sample and the amount of light transmitted through a blank. However, analysts are generally interested in the amount of light absorbed by a sample. Therefore, it is customary to convert transmittance to a measure of light absorption, called "absorbance". Absorbance is calculated based on the transmittance according to formula below [83]:

$$A = -\log(Transmittance) \tag{3.7}$$

Absorbance is also called "optical density" (OD). With modern spectrophotometers, you can adjust the instrument to either read out transmittance or to automatically convert the reading to an absorbance value.

An absorbance spectrum is a plot of the absorbance of a sample versus the wavelength of the light shined on the sample. To prepare such a spectrum, the absorbance of a single sample is measured successively at different wavelengths. Then, the absorbance of the sample is plotted with wavelength on the X-axis and absorbance is on the Y-axis. The resulting graph will have one or more peaks and valleys that are characteristic of that sample as shown in Fig. 3.15.

**Fig. 3.14** UV-Vis-NIR spectrophotometer.

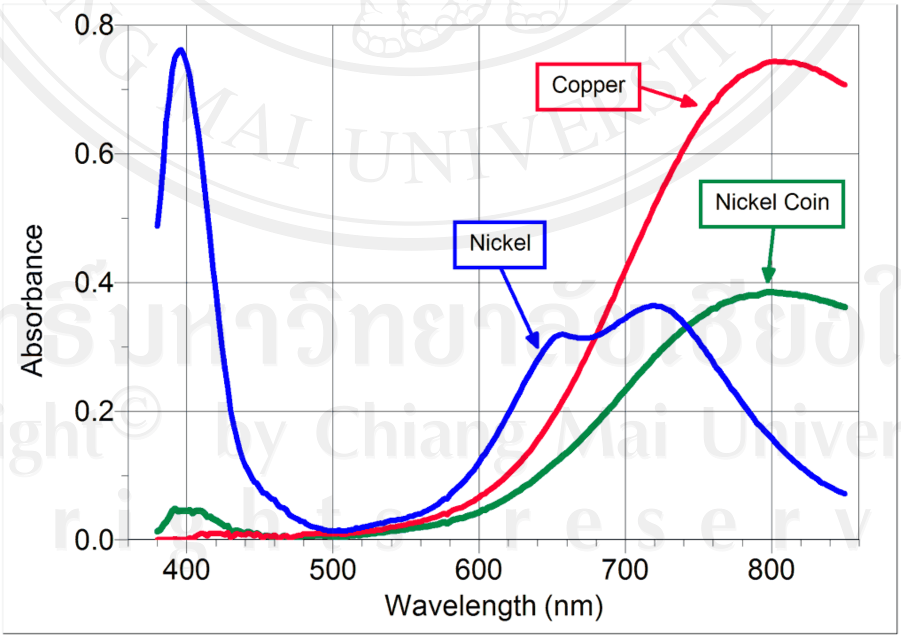

**Fig. 3.15** The absorbance spectrum of nickel, copper and nickel coin. [84]

### 3.2.5.2 Refractive index

The refractive index (or index of refraction) of a medium is a measure for how much the speed of light (or other waves such as sound waves) is reduced inside the medium. For example, typical soda-lime glass has a refractive index of 1.5, which means that in glass, light travels at 1/1.5 = 0.67 times the speed of light in a vacuum. Two common properties of glass and other transparent materials are directly related to their refractive index. First, light rays change direction when they cross the interface from air to the material, an effect that is used in lenses. Second, light reflects partially from surfaces that have a refractive index different from that of their surroundings.

The refractive index ($n$) of a medium is defined as the ratio of the phase velocity ($c$) of a wave phenomenon such as light or sound in a reference medium to the phase velocity ($\nu_p$), in the medium itself:

$$n = \frac{c}{\nu_p} \tag{3.8}$$

It is most commonly used in the context of light with vacuum as a reference medium, although historically other reference media (e.g. air at a standardized pressure and temperature) have been common. It is usually given the symbol $n$. In the case of light, it equals:

$$n = \sqrt{\varepsilon_r \ \mu_r} \tag{3.9}$$

Where $\varepsilon_r$ is the material's relative permittivity and $\mu_r$ is its relative permeability. For most materials, $\mu_r$ is very close to 1 at optical frequencies, therefore $n$ is approximately $\sqrt{\varepsilon_r}$ [85].

In the various theories of glass about the refractive index, scientists (Institute of Theoretical Chemistry, Shrewsbury, MA, USA) created a program and assembled glass property database for property predictions and calculations called “SciGlass”. In this research, we used this program to calculate the refractive index at 20 °C of the glass samples [86].

### 3.2.6 Measurement of electrical properties

#### 3.2.6.1 $LiNbO_3 \cdot SiO_2$ glass and glass-ceramic system

The capacitance (C) of the glasses and glass-ceramics (1-2 mm thick and 10 mm in diameter) was measured using impedance spectroscope (IM5d Zahner Elektrik, Kronach, Germany) (Fig. 3.16) at room temperature (about 25 °C) in the frequency (f) range of 10 kHz to 150 kHz with signal strength of 50 mV. The relative dielectric constant ($\varepsilon_r$) was calculated from the geometry of the sample and the capacitance [70]. Both surfaces were roughly polished using a gold-contacting paste as shown in Fig. 3.17.

$$\varepsilon = \frac{C \times s}{\varepsilon_0 \times A} \qquad \textbf{(3.10)}$$

Where $C$ is the capacitance of the bulk sample, $s$ is the thickness of the sample, $A$ is the area of the sample and $\varepsilon_0$ is free-space permittivity which value of $8.86 \times 10^{-12}$ F/m.

**Fig. 3.16** Impedance spectroscope (Kronach).

(a) (b)

**Fig. 3.17** Roughly polished sample (left side) and after using gold-contacting paste (right side): (a) top view and (b) side view.

#### 3.2.6.2 $LiNbO_3 \cdot SiO_2 \cdot Al_2O_3$ glass system

The capacitance (C) of the glass samples (1-2 mm thick and 6 mm in diameter) was measured using impedance spectroscope (Hewlett 4276A, LCZ meter, Japan) (Fig. 3.18) at room temperature (about 25 °C) in the frequency (f) range of 1 kHz to 1 MHz with signal strength of 1 V. The relative dielectric constant ($\varepsilon_r$) was calculated from the geometry of the sample and the capacitance (Equation 3.10). Both surfaces were fine polished into a mirror like form using alumina with a particle size of 1 μm by using silver (Ag)-contacting paste.

**Fig. 3.18** Impedance spectroscope (Hewlett).